Supplemental Appendix

Supplemental Methods

Mice

This study used male and female littermate wild-type and db/db mice between the ages of 16-20 weeks. At this age range db/db mice are obese and display glucose intolerance. The db/db mouse contains an autosomal recessive mutation in the leptin receptor (*Lepr*) gene. Mice homozygous for the mutation display hyperphagia and hyperglycemia. Db/db mice were initially obtained from the Jackson Laboratory (strain C57BL/6J-*Lepr*^{db}) and then bred locally. Homozygous db/db mice and wild-type littermates were used in this study. Animals were fed *ad libitum* and kept on a 12:12 h light-dark cycle. The diabetic phenotype was determined by oral glucose tolerance test.

Oral glucose tolerance test

Blood glucose levels were assessed by oral glucose tolerance test (OGTT). After 6 hours of fasting, mice were administered 50 mg of glucose by oral gavage. Blood samples were taken from the tail vein at regular intervals and blood glucose was measured with a glucometer (StatStrip Xpress®, Nova Biomedical, MA).

Osmotic pump insertion

For chronic GLP-1 studies db/db mice implanted with osmotic mini-pumps (Model 2004, Alzet) containing GLP-1 (7-36 amide). In control experiments db/db mice were implanted with pumps containing saline. GLP-1 was synthesized (Synpeptide Co) with the following amino acid sequence: His-Ala-Glu-Gly-Thr-Phe-Thr-Ser-Asp-Val-Ser-Ser-Tyr-Leu-Glu-Gly-Gln-Ala-Ala-Lys-Glu-Phe-Ile-Ala-Trp-Leu-Val-Lys-Gly-Arg-NH_2. Mice were anesthetized using isoflurane

inhalation (2-3%) and osmotic pumps were inserted subcutaneously via a 1-2 cm mid-scapular incision. Mice were given meloxicam (5 mg/kg) subcutaneously for post-operative analgesia.

Liraglutide treatment

For chronic liraglutide studies db/db mice were given subcutaneous injections of liraglutide or vehicle control once per day at approximately 9 AM each morning. Liraglutide was obtained from Synpeptide Co or from Bachem and had the following sequence: His-Ala-Glu-Gly-Thr-Phe-Thr-Ser-Asp-Val-Ser-Ser-Tyr-Leu-Glu-Gly-Gln-Ala-Ala-Lys(γ-Glupalmitoyl)-Glu-Phe-Ile-Ala-Trp-Leu-Val-Arg-Gly-Arg-Gly. Liraglutide was reconstituted in DMSO (1 mg/mL) and diluted in saline to a 10 μM stock solution. Vehicle consisted of a 3.7% DMSO solution in saline.

Insulin assay

Blood was collected via cardiac puncture from mice fasted for 4-6 hrs in tubes containing 0.04 mL of 7.5% EDTA solution. Whole blood was centrifuged at 1,000 rpm for 10 min to separate plasma, which was collected and frozen at −20 °C until experimental use. Plasma insulin was quantified using a mouse insulin ELISA assay (Mercodia Inc) according to manufacturer's instructions.

Blood pressure

Blood pressure was measured in conscious restrained mice using the CODA tail cuff system (Kent Scientific). Mice underwent 2 days of training prior to measurements. All blood pressure measurements were performed in a quiet dark room at a similar time of day. Data were analyzed using the CODA analysis software.

Echocardiography

Cardiac structure and function were assessed by echocardiography in mice anesthetized by isoflurane inhalation (2%) using a Vevo 3100 ultrasound system (Fujifilm VisualSonics, Canada).

***In vivo* electrophysiology**

A 1.2 French octapolar electrophysiology catheter containing 8 electrodes spaced 0.5 mm apart was used for intracardiac pacing experiments as we have described previously. Inducibility of AF was studied using 3 burst pacing protocols in the mid or high right atrium. The first protocol delivered a train of 45 pulses at a cycle length of 40 ms. After 2 min of rest the second protocol consisting of 80 pulses at a cycle length of 20 ms was applied. Finally, after an additional 2 min of rest, the third protocol consisting of 67 pulses at a cycle length of 20 ms was delivered. Pulse duration was 2 ms and each protocol was delivered 10 times. AF was defined as a rapid and irregular atrial rhythm (fibrillatory baseline in the ECG) with irregular RR intervals lasting at least 1 s on the surface ECG. Effective refractory periods (ERPs) were measured using a S1-S2 protocol where an 8 stimulus drive train (S1) at a fixed cycle length of 100 ms was delivered followed by an extra stimulus (S2) at a progressively shorter cycle length. AERP was defined as the shortest S1-S2 interval resulting in loss of capture of the P wave while AVERP was defined as the shortest S1-S2 interval resulting in a dropped QRS complex for AVERP measurements. Sinoatrial node recovery time (SNRT) was measured by delivering a 12 stimulus drive train at a cycle length of 100 ms. SNRT was defined as the time between the last stimulus in the drive train and the occurrence of the first spontaneous atrial beat (P wave). SNRT was corrected for heart rate (cSNRT) by subtracting the prestimulus RR interval from the measured SNRT. All ECG data were acquired using a Gould ACQ-7700 amplifier and Ponemah Physiology Platform software (Data Sciences International). Body temperature was maintained at 37 °C using a heating pad.

High-resolution optical mapping

To isolate atrial preparations, mice were administered a 0.2 mL intraperitoneal injection of heparin (1,000 IU/mL) to prevent blood clotting and were then anesthetized by isoflurane inhalation and sacrificed by cervical dislocation. Hearts were excised into Krebs solution (37°C) containing (in mM): 118 NaCl, 4.7 KCl, 1.2 KH_2PO_4, 25 $NaHCO_3$, 1 $CaCl_2$, 1 $MgCl_2$, 11 glucose and bubbled with 95% O_2/5% CO_2 to maintain a pH of 7.4. The atria were dissected away from the ventricles and pinned in a dish with the epicardial surface facing upward (toward the imaging equipment). The superior and inferior vena cavae were cut open so that the crista terminalis could be visualized, and the preparation could be pinned out flat with minimal tension.

The atrial preparation was superfused continuously with Krebs solution (37°C) bubbled with 95% O_2/5% CO_2 and allowed to equilibrate for ~10 min. The preparation was then incubated with the voltage sensitive dye RH-237 (15 μM; Biotium) for 15 min without superfusion. After the dye incubation period, superfusion was resumed with blebbistatin (10 μM; Cayman Chemical Company) added to the superfusate to suppress contractile activity and prevent motion artifacts. Experiments were performed in sinus rhythm so that the cycle length (ie, beating rate) of the atrial preparation was free to change as well as in atrial preparations paced at a fixed cycle length of 125 ms (8Hz) in order to study electrical conduction independently of changes in cycle length. The pacing electrode was placed near the opening of the superior vena cava. RH-237-loaded atrial preparations were illuminated with light from the X-Cite Xylis Broad Spectrum LED Illumination System (Excelitas Technologies) and filtered with a 520/35 nm excitation filter (Semrock). Emitted fluorescence was separated by a dichroic mirror (560 nm cutoff; Semrock) and filtered by a 715 nm long-pass emissions filter (Andover Corp.). Recordings were captured using a high-speed CMOS camera (MiCAM03-N256, SciMedia). Data were captured from an optical field of view of 11 x 11 mm at a frame rate of 1,000 frames/s using BrainVision software (BrainVision Inc). The spatial resolution was 42.5 x

42.5 μM for each pixel. Magnification was constant in all experiments and no pixel binning was used.

All optical data were analyzed using custom software written in MATLAB® (MathWorks). Pseudocolor electrical activation maps were generated from measurements of activation time at individual pixels as defined by assessment of dF/dt_{max} and background fluorescence was subtracted in all cases. Local conduction velocity (CV) was quantified specifically in the right atrial myocardium (within the right atrial appendage) and the left atrial myocardium (within the left atrial appendage). Activation times at each pixel from a 7 x 7 pixel array were determined and fit to a plane using the least squares fit method. The direction on this plane that is increasing the fastest represents the direction that is perpendicular to the wave front of electrical propagation and the maximum slope represents the inverse of the speed of conduction in that direction. With a spatial resolution of 42.5 x 42.5 μM per pixel, the area of the 7 x 7 pixel array was 297.5 x 297.5 μM. This approach allows assessment the maximum local CV vectors in the atrial region of interest. Optical APs were assessed by measuring the change in fluorescence as a function of time at individual pixels within the right and left atria.

Isolated of mouse atrial myocytes

Mice were administered a 0.2 mL intraperitoneal injection of heparin (1,000 IU/mL) to prevent blood clotting. Briefly, mice were anaesthetized using isoflurane inhalation and then sacrificed by cervical dislocation. The heart was excised into Tyrode's solution (35ºC) consisting of (in mM): 140 NaCl, 5.4 KCl, 1.2 KH_2PO_4, 1.0 $MgCl_2$, 1.8 $CaCl_2$, 5.55 glucose, and 5 HEPES, with pH adjusted to 7.4 with NaOH. Heparin was added to the Tyrode's solution to prevent blood clotting. The right or left atrial appendage was dissected from the heart, cut into strips and then equilibrated and washed in a 'low Ca^{2+}, Mg^{2+} free' solution containing (in mM): 140 NaCl, 5.4 KCl, 1.2 KH_2PO_4, 0.2 $CaCl_2$, 50 taurine, 18.5 glucose, 5 HEPES and 1 mg/mL bovine serum albumin (BSA), with pH adjusted to 6.9 with NaOH. Next, atrial tissue strips were enzymatically

digested for 30 min in 5 mL of 'low Ca^{2+}, Mg^{2+} free' solution that contained collagenase (type II, Worthington Biochemical Corporation), elastase (Worthington Biochemical Corporation) and protease (type XIV, Sigma Chemical Company). Next, the tissue was transferred to 2.5 mL of modified KB solution containing (in mM): 100 potassium glutamate, 10 potassium aspartate, 25 KCl, 10 KH_2PO_4, 2 $MgSO_4$, 20 taurine, 5 creatine, 0.5 EGTA, 20 glucose, 5 HEPES, and 0.1% BSA, with pH adjusted to 7.2 with KOH. Digested tissue strips were mechanically agitated using a wide-bore pipette. This procedure yielded individual right or left atrial myocytes that were stored in KB solution at room temperature and used for electrophysiology experiments within 6 hours of isolation.

Solutions and electrophysiological protocols

Stimulated action potentials (APs) were recorded using the whole cell patch-clamp technique. Myocytes were superfused with normal Tyrode's solution (22–23 °C) containing (in mM): 140 NaCl, 5 KCl, 1 $MgCl_2$, 1 $CaCl_2$, 10 HEPES, and 5 glucose, with pH adjusted to 7.4 with NaOH. The pipette filling solution contained (in mM): 135 KCl, 0.1 $CaCl_2$, 1 $MgCl_2$, 5 NaCl, 10 EGTA, 4 Mg-ATP, 6.6 Na-phosphocreatine, 0.3 Na-GTP and 10 HEPES, with pH adjusted to 7.2 with KOH. The resting membrane potential was corrected for a liquid junction potential of 4.6 mV.

For recording I_{Na} atrial myocytes were superfused with a modified Tyrode's solution (22–23 °C) containing the following (in mM): 130 CsCl, 5 NaCl, 5.4 TEA-Cl, 1 $MgCl_2$, 1 $CaCl_2$, 10 HEPES, 5.5 glucose, (pH 7.4, adjusted with CsOH). Nitrendipine (10 μM) was added to the superfusate to block $I_{Ca,L}$. The pipette solution for I_{Na} contained (in mM): 120 CsCl, 5 NaCl, 1 $MgCl_2$, 0.2 $CaCl_2$, 10 HEPES, 5 MgATP, 0.3 Na-GTP, 5 BAPTA (pH 7.2, adjusted with CsOH). I_{Na} was recorded using 50 ms voltage clamp steps between −100 and 10 mV from a holding potential of −120 mV.

I_{Na} activation kinetics were determined by calculating chord conductance (G) with the equation $G = I/(V_m - E_{rev})$, where V_m represents the depolarizing voltages and E_{rev} is the reversal potential measured from the current-voltage relationships of $I_{Ca,L}$ or I_{Na}. Maximum conductance (G_{max}) and $V_{1/2}$ of activation ($V_{1/2(act)}$) for $I_{Ca,L}$ and I_{Na} were determined using the following function: $G = [(V_m - V_{rev})][G_{max}][-1/[(1 + \exp((V_m - V_{1/2})/k))+1]]$.

I_{Na} steady-state inactivation kinetics were measured using 500 ms prepulse voltage clamp steps between −120 and −30 mV from a holding potential of −120 mV followed by a 20 ms test pulse to −20 mV. Normalized peak currents were plotted as a function of the prepulse potential and the resulting curve was fitted with the Boltzmann function $h = 1/[1 + \exp[V_{1/2} - V]/k]$. These data were used to measure the voltage at which 50% of channels are inactivated ($V_{1/2(inact)}$).

Total potassium currents (I_K) were recorded in the whole cell configuration of the patch clamp technique using the same Tyrode's solution and pipette solutions used to record APs. To record total potassium currents (no prepulse), cells were held at −80 mV then I_K was recorded using a series of voltage clamp steps (500 ms duration) between −120 and +80 mV in 10 mV increments. To record potassium currents with an inactivating prepulse (to inactivate I_{to}), cells were given a 200 ms repulsed to −40 mV immediately followed by 500 ms voltage clamp steps from −120 to +80 mV from a holding potential of −80 mV. For these recordings with and without a prepulse, I_K was measured at the peak current for each voltage step. I_{to} was calculated as the difference current between the recordings with and without a prepulse. I_{Kur}, as carried by $K_V1.5$ channels, was measured as the component of I_K sensitive to 4-aminopyradine (4-AP; 100 μM). The voltage clamp protocol for measuring I_{Kur} included a prepulse to −40 mV for 200 ms to inactivate I_{to} immediately followed by a 500 ms step to +30 mV before returning to a holding potential of −80 mV. Peak currents at baseline, in the presence of 4-AP, and after washout were measured.

AP duration variability was assessed using Poincaré plot analysis. From these plots the SDs (SD1 and SD2) for APD_{70} were calculated using the following equations: $SD1^2 = 1/2[SD(APD_n - APD_{n+1})]^2$ and $SD2^2=2[SD(APD)]^2 - 1/2[SD(APD_n - APD_{n+1})]$.

Micropipettes were pulled from borosilicate glass (with filament, 1.5 mm OD, 0.75 mm ID, Sutter Instrument Company) using a Flaming/Brown pipette puller (model p-87, Sutter Instrument Company). The resistance of these pipettes was 4–8 MΩ when filled with pipette solution. Micropipettes were positioned using a micromanipulator (Burleigh PCS-5000 system) mounted on the stage of an inverted microscope (Olympus IX71). Seal resistance was 2 – 15 GΩ and access resistances were 5–15 MΩ following rupture of the sarcolemma. Series resistance compensation to 85% using an Axopatch 200B amplifier (Molecular Devices). Data were digitized using a Digidata 1440 and pCLAMP 10 software (Molecular Devices) and stored on computer for analysis. No junction potential corrections were applied in our analyses. All patch-clamp studies were conducted at room temperature.

Quantitative PCR

Quantitative gene expression was measured in the right and left atria. Primers for *Kcnd2* (K_V4.2), *Kcnd3* (K_V4.3), *Kcnip2* (KChIP2), *Kcna5* (K_V1.5), *Col1a* (collagen type I), *Col3a* (collagen type III), and hypoxanthine phosphoribosyltransferase (*Hprt1*;reference gene) were used. Primer sequences are listed in Supplemental Table S7 below.

Total RNA was isolated from right or left atrial appendages using a PureZOL™ RNA Isolation Reagent and the Aurum™ Total RNA Fatty and Fibrous Tissue Kit (Bio-Rad Laboratories) as per kit instructions. RNA samples were eluted from the spin column in 40 µL elution buffer. RNA yield and purity were assessed using a Nanodrop. All samples had a A_{260}/A_{280} of over 2.0 and therefore were free of DNA contamination. Next, cDNA (5 ng/µL) was synthesized using the iScript™ cDNA Synthesis Kit (Bio-Rad Laboratories). Reactions were performed in a Bio-Rad MyCycler thermal cycler using the following protocol: 5 min of priming at

25 °C followed by reverse transcription for 30 min at 42 °C then 5 min at 85 °C to inactivate reverse transcriptase.

All qPCR reactions were run in duplicate in 10 µL reactions that contained the following: 4 µL sample cDNA, 5.6 µL GoTaq® qPCR Master Mix (Promega), and 0.4 µL primers. Primers were reconstituted to a final concentration of 100 µM with nuclease free water and stored at −20 °C until use. Primers were diluted to 10 µM for qPCR reactions. RT-qPCR reactions were performed using the CFX386 Touch™ Real-Time PCR Detection System (Bio-Rad) using the following protocol: Taq polymerase was activated for 2 min at 95 °C followed by 39 cycles of denaturing for 15 s at 95 °C, annealing for 30 s at 60 °C, and extension for 30 s at 72 °C. This was followed by melt curve analysis from 65-95 °C in 0.5 °C increments. Data were analyzed using the $2^{-\Delta\Delta C_T}$ method using the CFX Manager Software version 3.1 (Bio-Rad).

Western blotting

Protein samples were extracted from the left atrial appendage. Tissue was cooled in liquid nitrogen, ground into a powder, and then incubated for 1 hour with ice-cold modified RIPA buffer that contained (in mM): 50 mM Tris, 150 mM NaCl, 25 mM sucrose, 1 mM EDTA, 1% Triton, 0,1% SDS. Protease inhibitor cocktail (Sigma-Aldrich) and 0.5 mM DTT (1,4-Dithiothreitol, Roche) were added to prevent protein degradation. Next, preparations were centrifuged for 10 min at 10,000 rpm at 4 °C and protein concentrations were measured using the Bio-Rad DC™ Protein Assay Kit II (Bio-Rad Laboratories). For K_v4.2, K_v4.3, and K_v1.5 Western blot experiments, protein samples (20 µg/lane) were separated by 7.5% SDS-polyacrylamide gels (SDS-PAGE) and transferred onto a BioTrace™ NT Nitrocellulose Transfer Membrane (VWR). For KChIP2 Western blot experiments, a protein concentration of 40 µg/lane was used and proteins were separated on a 10% SDS-PAGE gel. The membrane was blocked for 1 hour at room temperature with 1% casein in Tris-buffered saline (TBS; Bio-Rad Laboratories). Blots were incubated overnight at 4 °C with rabbit-raised primary antibodies to

K_v4.2 (1:500, Alomone Labs), K_v4.3 (1:1,000, Alomone Labs), K_v1.5 (1:500, Alomone Labs) or KChIP2 (1:500, Alomone Labs). The Western blot membranes were then washed 3 times for 10 min in 1% TBST (TBS with 1% Tween 20 (Bio-Rad Laboratories)) before secondary antibody binding. Membranes were incubated with goat anti-rabbit IgG StarBright Blue 700 (1:2,500, Bio-Rad Laboratories) fluorescent secondary antibodies for 1 hour at room temperature. In K_v4.3, KChIP2, and K_v1.5 experiments, membranes were simultaneously incubated with hFAB Rhodamine Anti-GAPDH IgG (1:5,000, Bio-Rad Laboratories) as a primary anti-GAPDH antibody was not used. Following incubation, the membrane was washed 3 times for 10 min with 1% TBST before imaging. All Western blot membranes were imaged using the ChemiDoc™ MP Imaging System (Bio-Rad Laboratories). Protein expression was normalized to GAPDH.

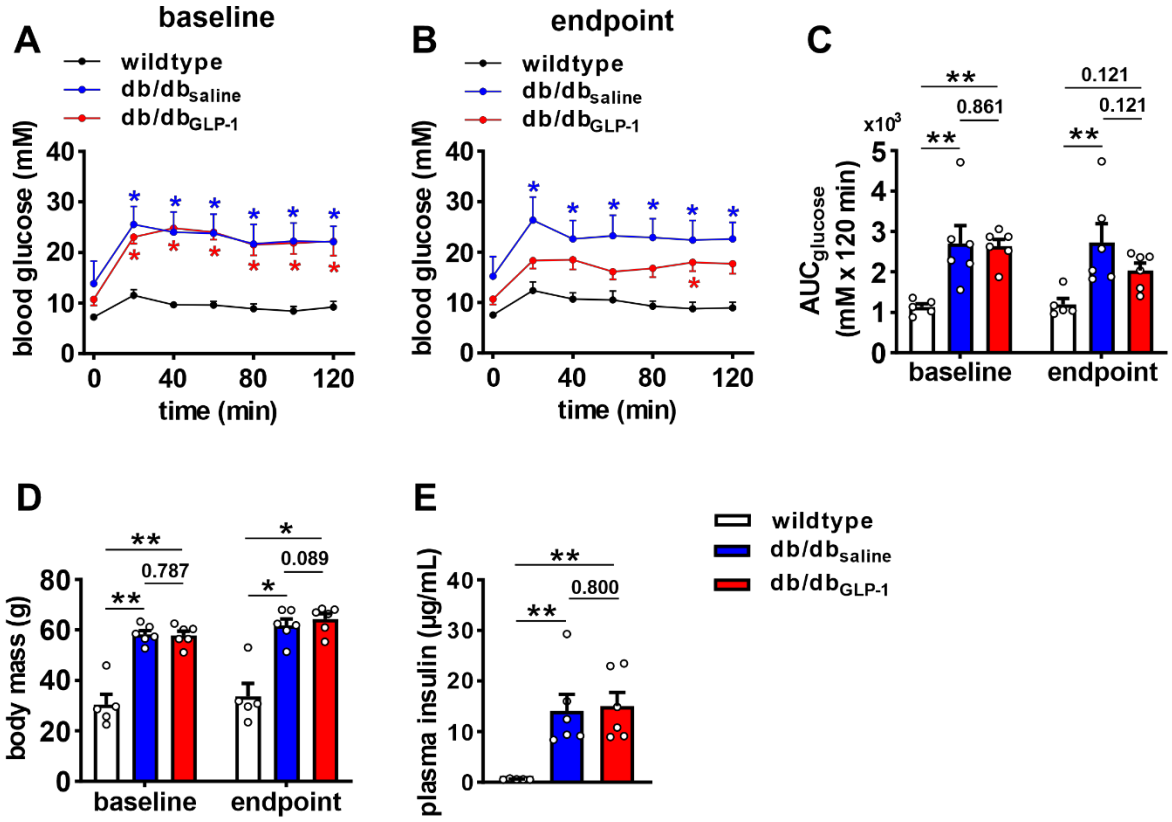

Supplemental Figure 1: Blood glucose, body mass, and plasma insulin in db/db mice treated with GLP-1 for 4 weeks. (**A and B**) Oral glucose tolerance test in wild-type, db/db$_{saline}$, and db/db$_{GLP-1}$ mice at baseline (**A**) and after 4 weeks of GLP-1 (or saline) infusion (**B**). *P < 0.05 vs wild type by two-way repeated measures ANOVA with Holm-Sidak post hoc test. (**C**) Area under the curve (AUC$_{glucose}$) for the data in panels A and B. Data analyzed by two-way repeated measures ANOVA with Holm-Sidak post hoc test. (**D**) Body mass in wild-type, db/db$_{saline}$, and db/db$_{GLP-1}$ mice at baseline and after 4 weeks of GLP-1 (or saline) treatment. Data analyzed by two-way repeated measures ANOVA with Holm-Sidak post hoc test. For panels A-D n = 5 wild-type, 6 db/db$_{saline}$, and 6 db/db$_{GLP-1}$ mice. (**E**) Plasma insulin levels in wild-type, db/db$_{saline}$, and db/db$_{GLP-1}$ mice after 4 weeks of GLP-1 (or saline) treatment. Data analyzed by one-way ANOVA with Holm-Sidak post hoc test; n = 5 mice per group.

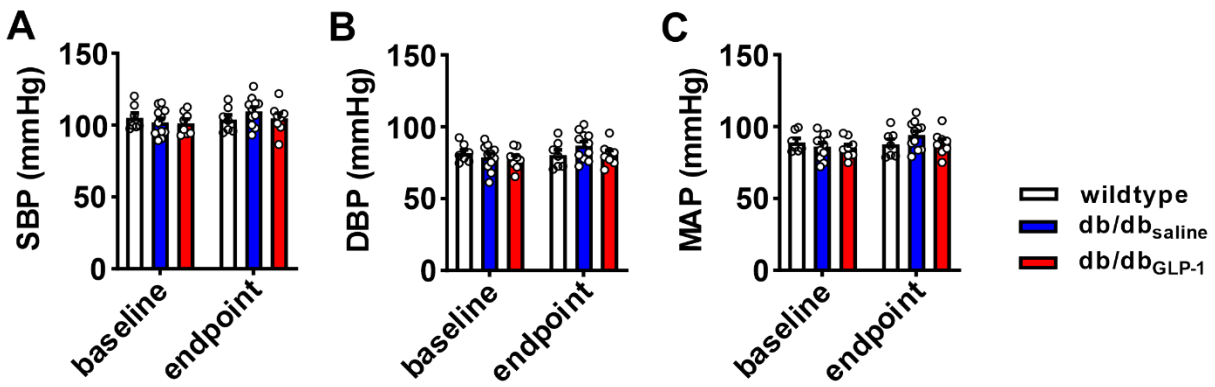

Supplemental Figure 2: Blood pressure in db/db mice treated chronically with GLP-1. (**A-C**) systolic (SBP; **A**), diastolic (DBP, **B**) and mean arterial (MAP, **C**) pressures in wild-type, db/db_{saline}, and db/db_{GLP-1} mice at baseline and after 4 weeks of GLP1 (or saline) infusion. There were no differences in blood pressure between groups or at different time points. Data analyzed by two-way repeated measures ANOVA with Holm-Sidak post hoc test; n = 7 wild-type, 11 db/db_{saline}, and 8 db/db_{GLP-1} mice.

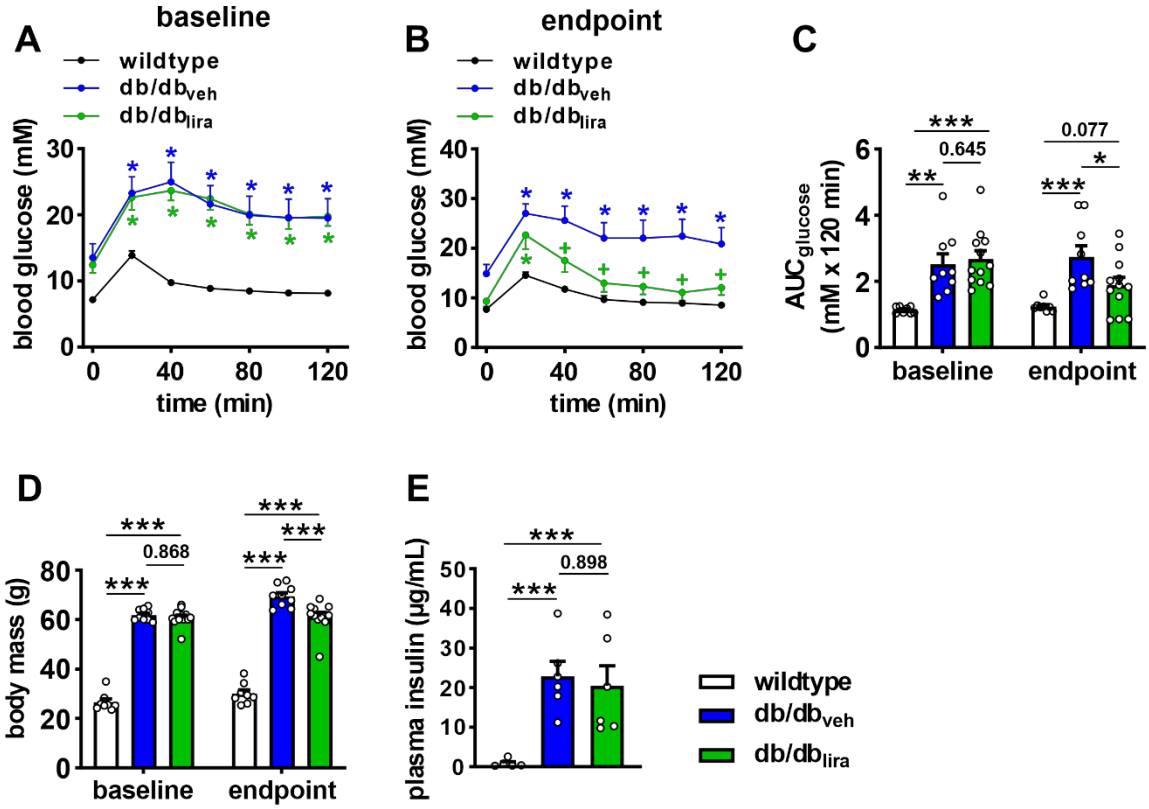

Supplemental Figure 3: Blood glucose, body mass, and plasma insulin in db/db mice treated with liraglutide for 4 weeks. (**A and B**) Oral glucose tolerance test in wild-type, db/db$_{veh}$, and db/db$_{lira}$ mice at baseline (**A**) and after 4 weeks of daily liraglutide (or vehicle) injections (**B**). $^{*}P < 0.05$ vs wild type, $^{+}P < 0.05$ vs db/db$_{veh}$ by two-way repeated measures ANOVA with Holm-Sidak post hoc test. (**C**) Area under the curve (AUC$_{glucose}$) for the data in panels A and B. Data analyzed by two-way repeated measures ANOVA with Holm-Sidak post hoc test. (**D**) Body mass in wild-type, db/db$_{veh}$, and db/db$_{lira}$ mice at baseline and after 4 weeks of liraglutide (or vehicle) injections. Data analyzed by two-way repeated measures ANOVA with Holm-Sidak post hoc test. For panels A-D n = 8 wild-type, 9 db/db$_{veh}$, and 12 db/db$_{lira}$ mice. (**E**) Plasma insulin levels in wild-type, db/db$_{veh}$, and db/db$_{lira}$ mice after 4 weeks of liraglutide (or vehicle) injections. Data analyzed by one-way ANOVA with Holm-Sidak post hoc test; n = 6 mice per group.

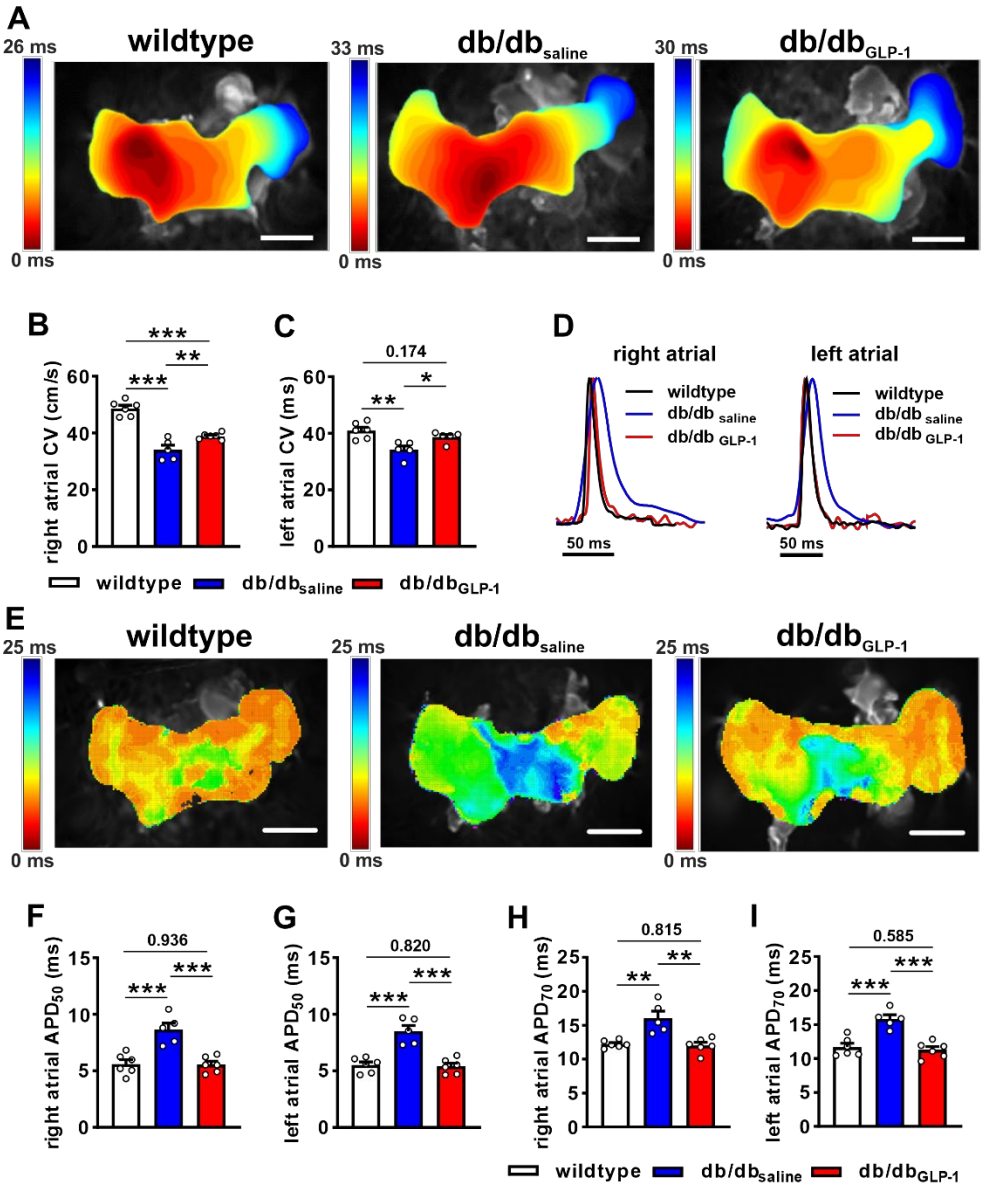

Supplemental Figure 4: Effects of chronic GLP-1 on atrial conduction and atrial optical action potential morphology in db/db hearts in sinus rhythm. (**A**) Representative activation maps in isolated atrial preparations from wild-type, db/db$_{saline}$, and db/db$_{GLP-1}$ mice in sinus rhythm. Right atrial appendage is on the left side of the image. Color scale indicates total conduction time across the preparation. Scale bar = 2 mm. (**B and C**) Summary of right atrial (**B**) and left atrial (**C**) conduction velocity (CV) in wild-type, db/db$_{saline}$, and db/db$_{GLP-1}$ mice. (**D**) Representative right atrial and left atrial optical action potentials in isolated atrial preparations from wild-type, db/db$_{saline}$, and db/db$_{GLP-1}$ mice. (**E**) Representative action potential duration maps at 50% repolarization time (APD_{50}) in atrial preparations from wild-type, db/db$_{saline}$, and db/db$_{GLP-1}$ mice. Scale bar = 2 mm. (**F and G**) Summary of right (**F**) and left (**G**) atrial APD_{50} in atrial preparations from wild-type, db/db$_{saline}$, and db/db$_{GLP-1}$ mice. (**H and I**) Summary of right (**H**) and left (**I**) atrial APD_{70} in atrial preparations from wild-type, db/db$_{saline}$, and db/db$_{GLP-1}$ mice. All summary data analyzed by one-way ANOVA with Holm-Sidak post hoc test; n = 5-6 atrial preparations per group.

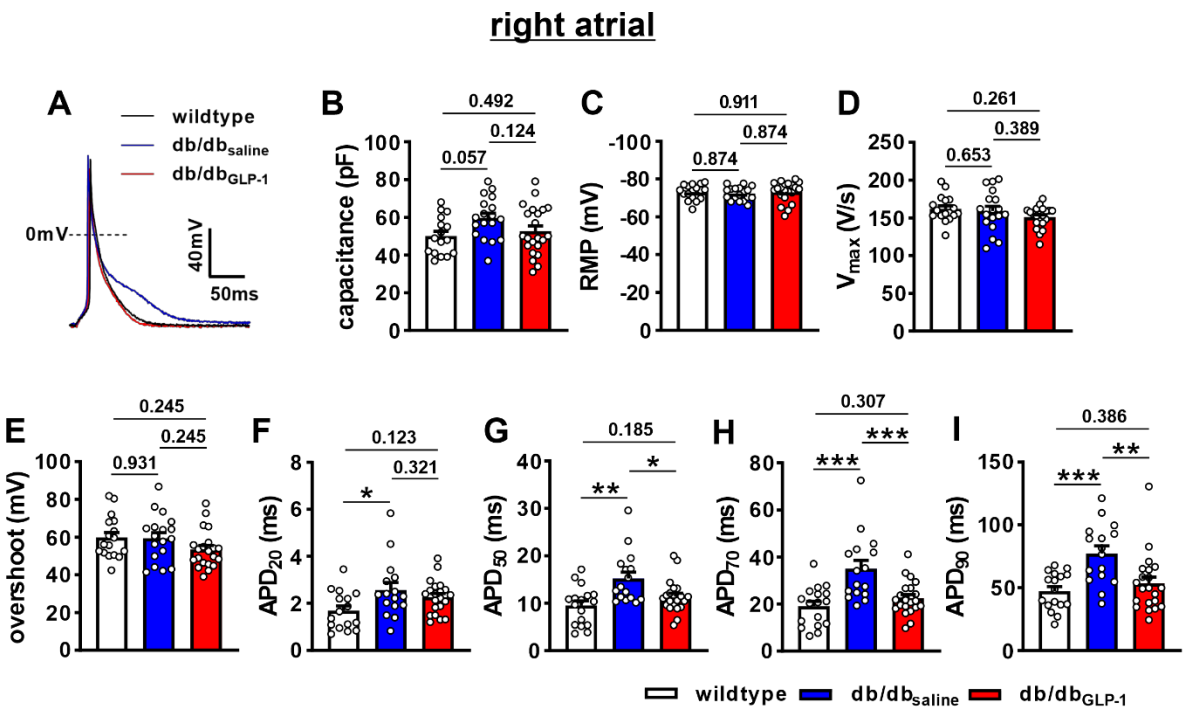

Supplemental Figure 5: Effects of chronic GLP-1 on action potential morphology in isolated right atrial myocytes in db/db mice. (**A**) Representative stimulated action potentials in right atrial myocytes isolated from wild-type, db/db$_{saline}$, and db/db$_{GLP-1}$ mice. (**B-I**) Summary data for cell capacitance (**B**), resting membrane potential (RMP, **C**), AP upstroke velocity (V_{max}, **D**), overshoot (**E**), APD_{20} (**F**), APD_{50} (**G**), APD_{70} (**H**), and APD_{90} (**I**) in isolated right atrial myocytes from wild-type, db/db$_{saline}$, and db/db$_{GLP-1}$ mice. Data analyzed by one-way ANOVA with Holm-Sidak post hoc test; n = 17 myocytes from 5 mice for wild type, 18 myocytes from 7 mice for db/db$_{saline}$, and 21 cells from 8 mice for db/db$_{GLP-1}$.

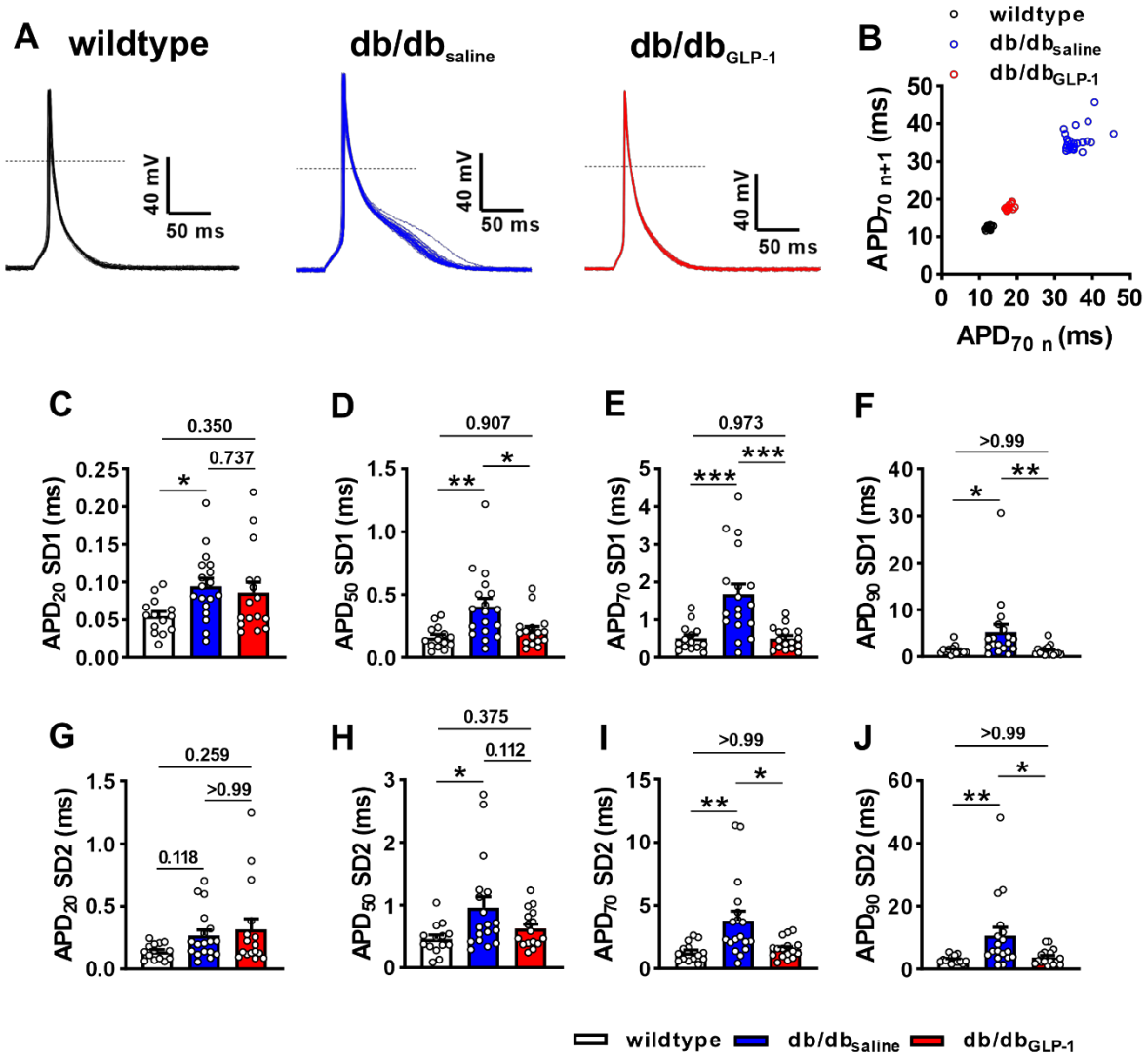

Supplemental Figure 6: Effects of chronic GLP-1 on action potential heterogeneity in right atrial myocytes in db/db mice. (**A**) Representative overlays of stimulated action potentials in isolated right atrial myocytes from wild-type, db/db$_{saline}$, and db/db$_{GLP-1}$ mice. (**B**) Representative Poincaré plot for APD$_{70}$ for stimulated APs in right atrial myocytes from wild-type, db/db$_{saline}$, and db/db$_{GLP-1}$ mice. (**C-F**) Summary of SD 1 (SD1) for APD$_{20}$ (**C**), APD$_{50}$ (**D**), APD$_{70}$ (**E**), and APD$_{90}$ (**F**) for isolated right atrial myocytes. (**G-J**) Summary of SD 2 (SD2) for APD$_{20}$ (**G**), APD$_{50}$ ($_{H}$), APD$_{70}$ (**I**) and APD$_{90}$ (**J**) for isolated right atrial myocytes. For panels C-J data analyzed by one-way ANOVA with Holm-Sidak post hoc test; n = 14 myocytes from 5 mice for wild type, 18 myocytes from 7 mice for db/db$_{saline}$, and 16 myocytes from 7 mice for db/db$_{GLP-1}$.

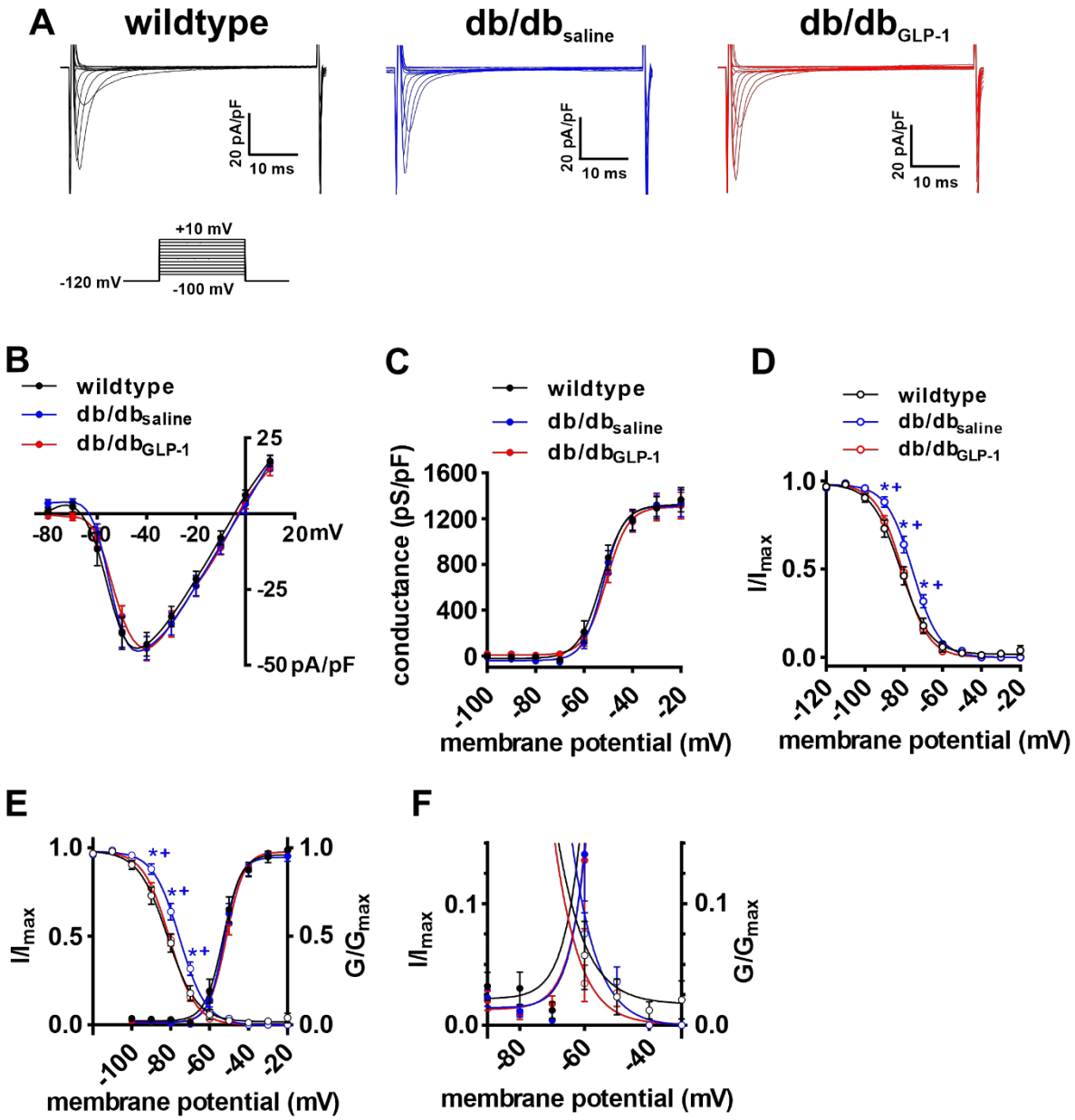

Supplemental Figure 7: Effects of chronic GLP-1 on Na^+ current in isolated right atrial myocytes from db/db mice. (**A**) Representative I_{Na} recordings in isolated right atrial myocytes from wild-type, db/db_{saline}, and db/db_{GLP-1} mice. Voltage clamp protocol shown below recordings. (**B-D**) I_{Na} IV curves (**B**), steady-state activation curves (**C**), and steady-state inactivation curves (**D**) in right atrial myocytes from wild-type, db/db_{saline}, and db/db_{GLP-1} mice. Data analyzed by two-way repeated measures ANOVA with Holm-Sidak post hoc test. There were no differences between groups in panels B and C. For panel D $^*P < 0.05$ vs wild type, $^+P < 0.05$ vs db/db_{GLP-1}. n = 10 myocytes from 3 mice for wild type, 11 myocytes from 4 mice for db/db_{saline}, and 11 myocytes from 3 mice for db/db_{GLP-1}. (**E**) Combined plots of normalized steady-state activation (G/G_{max}) and inactivation (I/I_{max}) in right atrial myocytes from wild-type, db/db_{saline}, and db/db_{GLP-1} mice. (**F**) Magnified view of steady state activation and inactivation curves illustrating window currents in wild-type, db/db_{saline}, and db/db_{GLP-1} right atrial myocytes. Refer to Supplemental Table 6 for additional analysis.

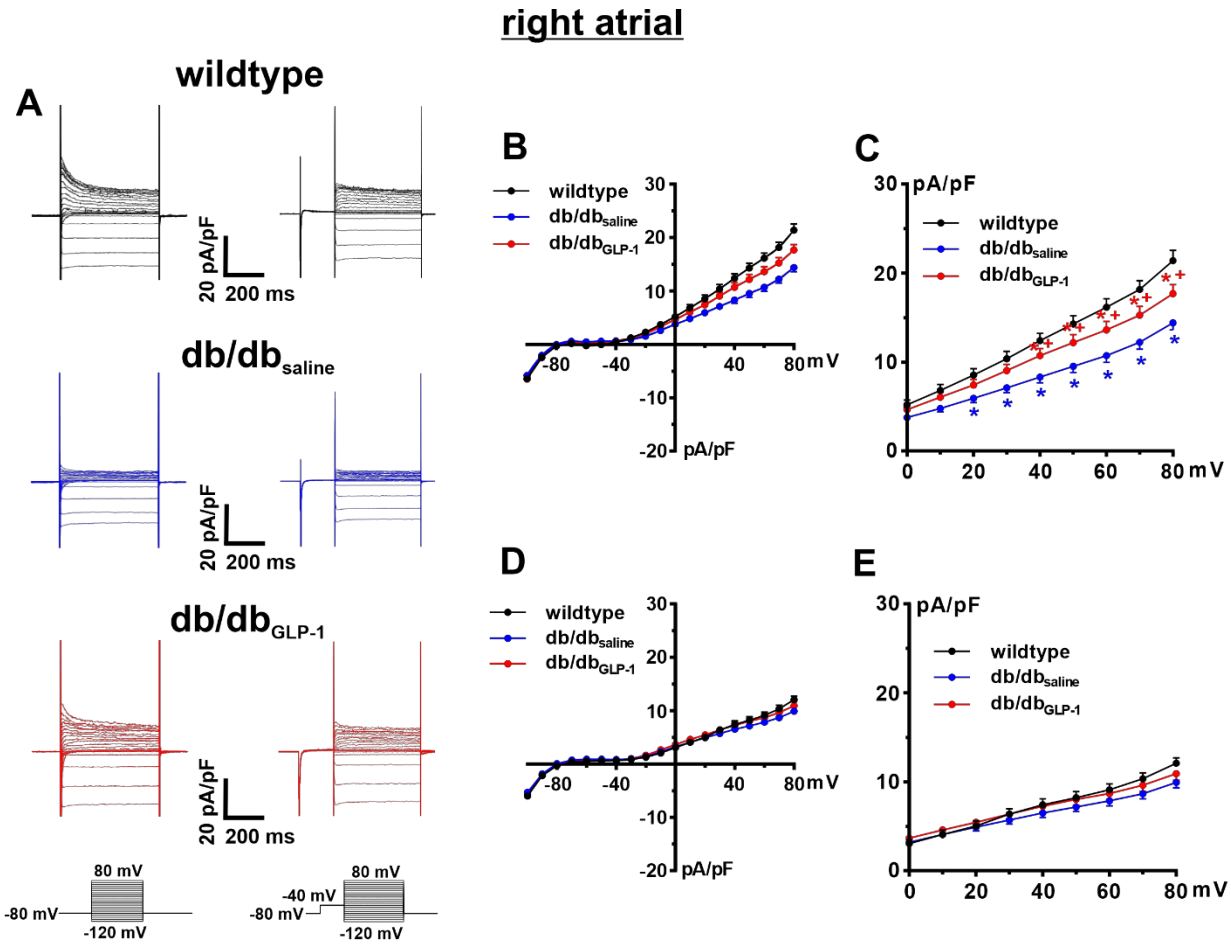

Supplemental Figure 8: Effects of chronic GLP-1 on K^+ currents in isolated right atrial myocytes in db/db mice. (**A**) Representative I_K recordings for total I_K (left) and I_K after an inactivating prepulse to −40 mV (right) in right atrial myocytes isolated from wild-type, db/db$_{saline}$, and db/db$_{GLP-1}$ mice. Voltage clamp protocols shown below recordings. (**B**) I_K IV curves measured at the peak of the total I_K recordings. (**C**) I_K IV curves (same data as panel B) showing repolarizing I_K at membrane potentials positive to 0 mV. (**D**) I_K IV curves measured at the peak of the I_K recordings after an inactivating prepulse. (**E**) I_K IV curves after an inactivating prepulse (same data as panel D) showing I_K at membrane potentials positive to 0 mV. For panel C $^*P < 0.05$ vs wild type, $^+P < 0.05$ vs db/db$_{saline}$. For panel E there were no differences between groups. Data analyzed by two-way repeated measures ANOVA with Holm-Sidak post hoc test; n = 14 myocytes from 5 mice for wild type, 16 myocytes from 8 mice for db/db$_{saline}$, and 25 myocytes from 9 mice for db/db$_{GLP-1}$. Statistical symbols shown only on panel C for clarity.

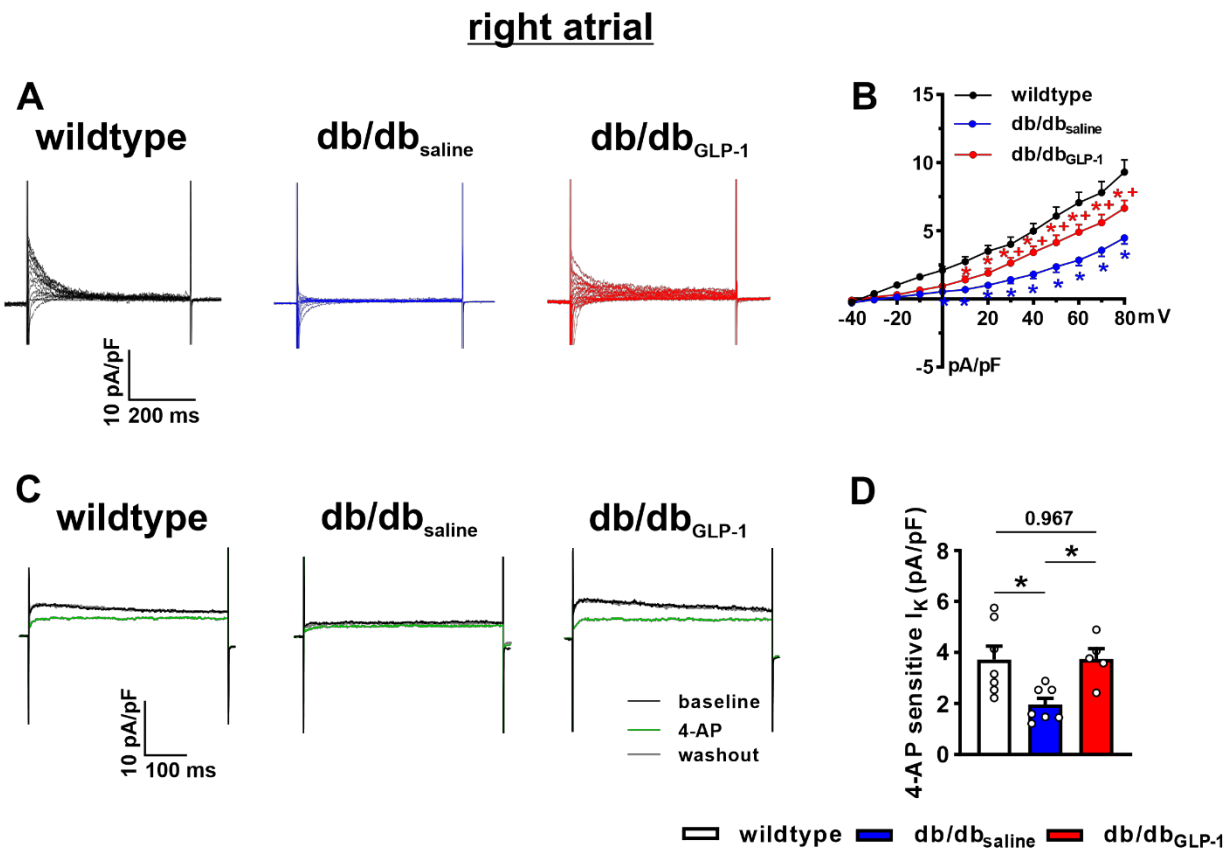

Supplemental Figure 9: Effects of chronic GLP-1 on I_{to} and 4-aminopyridine sensitive I_{Kur} in isolated right atrial myocytes in db/db mice. (**A**) Representative I_{to} recordings in isolated right atrial myocytes from wild-type, db/db_{saline}, and db/db_{GLP-1} mice generated by digitally subtracting the I_K recordings with and without a prepulse as seen in Supplemental Figure 8. (**B**) I_{to} IV curves measured as the difference current between I_K recordings with and without a prepulse as shown in Supplemental Figure 8. $^{*}P < 0.05$ vs wild type; $^{+}P < 0.05$ vs db/db_{GLP-1} by mixed-effects ANOVA with Holm-Sidak post hoc test; n =14 myocytes from 5 mice for wild type, 16 myocytes from 8 mice for db/db_{saline}, and 25 myocytes from 9 mice for db/db_{GLP-1}. (**C**) Representative I_K recordings at +30 mV showing the effects of 4-aminopyridine (4-AP; 100 μM), which inhibits $K_V1.5$-mediated I_{Kur}, in isolated right atrial myocytes from wild-type, db/db_{saline}, and db/db_{GLP-1} mice. (**D**) Summary of amplitude of 4-AP sensitive I_K in isolated right atrial myocytes from wild-type, db/db_{saline}, and db/db_{GLP-1} mice. Data analyzed by one-way ANOVA with Holm-Sidak post hoc test; n = 7 myocytes from 2 mice for wild type, 7 myocytes from 2 mice for db/db_{saline}, and 5 myocytes from 2 mice for db/db_{GLP-1}.

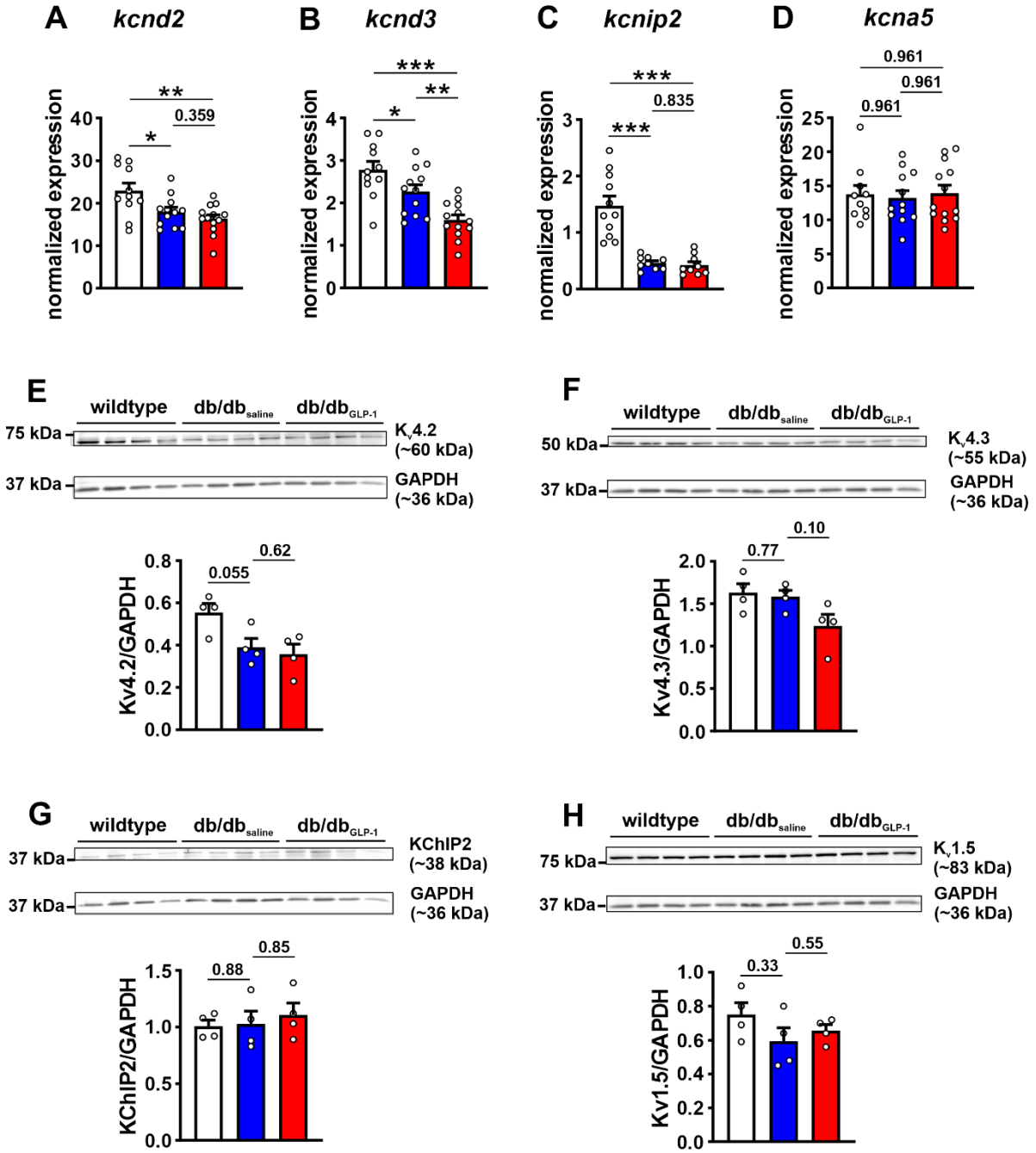

Supplemental Figure 10: Effects of chronic GLP-1 on left atrial K^+ channel mRNA and protein expression in db/db mice. (**A-D**) mRNA expression for *Kcnd2* (**A**), *Kcnd3* (**B**), *Kcnip2* (**C**), and *Kcna5* (**D**) in the left atrium in wild-type, db/db_{saline}, and db/db_{GLP-1} mice. Data analyzed by one-way ANOVA with Holm-Sidak post hoc test; n = 11 wild-type, 12 db/db_{saline}, and 13 db/db_{GLP-1} mice. (**E-F**) Representative Western blots and summary protein expression for $K_v4.2$ (**E**), $K_v4.3$ (**F**), KChIP2 (**G**), and $K_v1.5$ (**H**). Data analyzed by one-way ANOVA with Holm-Sidak post hoc test; n = 4 atria per group. Uncropped Western blots provided in Supplemental Figure 13.

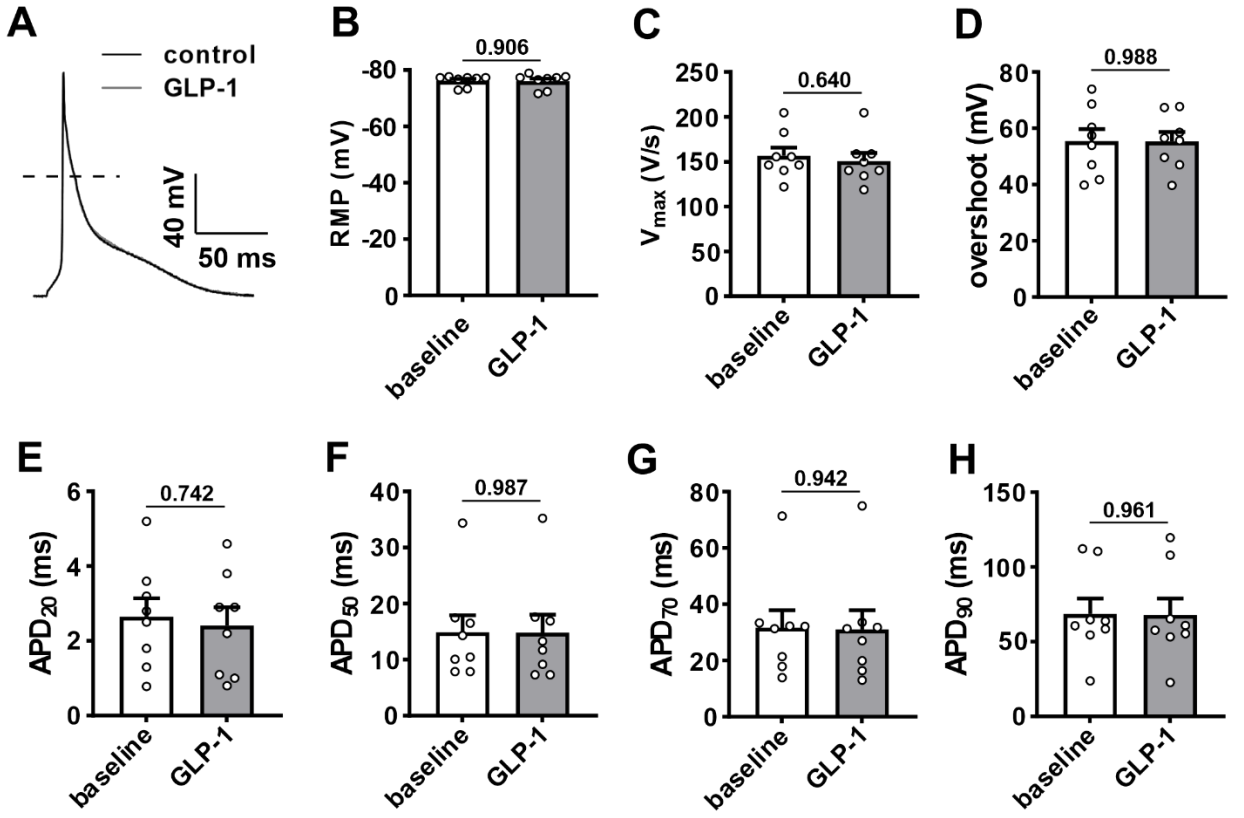

Supplemental Figure 11: Effects of acute GLP-1 on action potential morphology in isolated atrial myocytes from db/db mice. (**A**) Representative stimulated atrial action potentials in control conditions and after 5-10 min of acute superfusion with GLP-1 (100 nM). (**B-C**) Summary of the effects of acute GLP-1 on RMP (**B**), V_{max} (**C**), overshoot (**D**), APD_{20} (**E**), APD_{50} (**F**), APD_{70} (**G**), and APD_{90} (**H**) in isolated atrial myocytes from db/db mice. Data analyzed by Student's *t-test*, n = 8 myocytes from 3 mice.

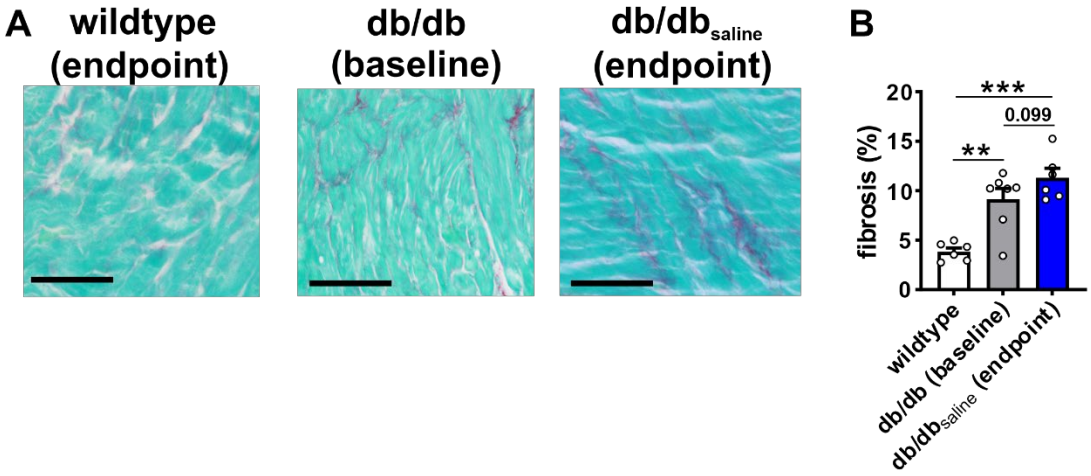

Supplemental Figure 12: Left atrial fibrosis in db/db mice. (**A**) Representative images showing patterns of interstitial fibrosis (red staining) in the left atria in wild-type mice at endpoint (ie, at time of functional studies), in db/db mice at baseline (ie, the timepoint at which GLP-1/saline infusion started), and in db/db$_{saline}$ mice at endpoint (ie, at time of functional studies). Scale bar = 50 μM. (**B**) Summary of left atrial fibrosis. Data analyzed by one-way ANOVA with Holm-Sidak post hoc test. n = 6 for wild-type endpoint, 7 for db/db$_{baseline}$, and 6 for db/db$_{saline}$ endpoint. Images and summary data for wild-type endpoint and db/db$_{saline}$ endpoint are the same as in Figure 9.

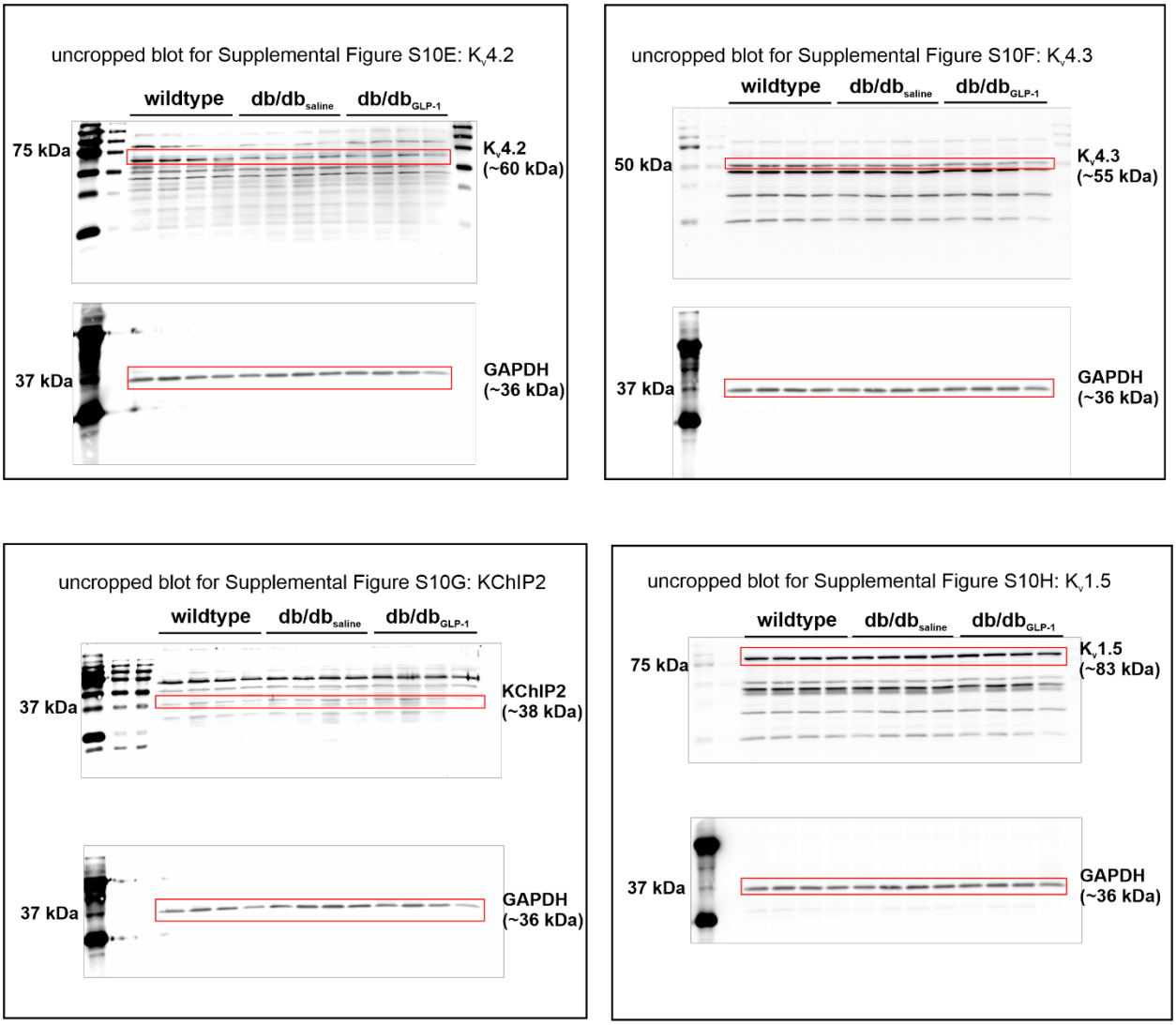

Supplemental Figure 13: Uncropped gels for Western blots.

Supplemental Table 1: Echocardiography measures in db/db mice treated with GLP-1 for 4 weeks.

	wild type	db/db_{saline}	db/db_{GLP-1}	*P* value db/db_{saline} vs wild type	*P* value db/db_{GLP-1} vs db/db_{saline}
n	11	6	8		
LVAWd (mm)	0.88 ± 0.05	0.86 ± 0.05	0.99 ± 0.04	0.98	0.21
LVPWd (mm)	0.92 ± 0.04	0.85 ± 0.05	0.97 ± 0.05	0.51	0.22
LVIDd (mm)	4.52 ± 0.07	4.47 ± 0.11	4.14 ± 0.13	0.95	0.12
LVAWs (mm)	1.32 ± 0.07	1.45 ± 0.08	1.62 ± 0.05	0.21	0.21
LVPWs (mm)	1.23 ± 0.04	1.29 ± 0.06	1.43 ± 0.06	0.46	0.16
LVIDs (mm)	3.26 ± 0.10	2.86 ± 0.09	2.53 ± 0.13	0.052	0.072
LVVd (µL)	68.2 ± 2.9	68.6 ± 2.1	68.7 ± 5.3	>0.99	>0.99
LVVs (µL)	35.5 ± 2.2	31.5 ± 1.4	32.0 ± 3.3	0.69	0.92
EF (%)	47.8 ± 2.6	54.1 ± 1.2	54.3 ± 2.0	0.21	0.96
SV (µL)	32.7 ± 2.4	37.1 ± 1.1	36.9 ± 2.4	0.48	0.97
LA $area_{max}$ (mm^2)	5.01 ± 0.33	6.79 ± 0.58	5.43 ± 0.51	0.039	0.12
LA $area_{min}$ (mm^2)	2.98 ± 0.40	3.27 ± 0.43	3.81 ± 0.33	0.64	0.64
RA $area_{max}$ (mm^2)	4.38 ± 0.31	5.42 ± 0.56	4.28 ± 0.38	0.21	0.21
RA $area_{min}$ (mm^2)	2.48 ± 0.32	3.09 ± 0.43	3.38 ± 0.57	0.59	0.67

n, number of mice, LVAW, left ventricular anterior wall thickness; LVPW, left ventricular posterior wall thickness; LVID, left ventricular internal diameter; LVV, left ventricular volume. LVAW, LVPW, LVID and LVV measurements were made during systole (s) and diastole (d). SV, stroke volume; EF, ejection fraction; LA $area_{max}$, maximum left atrial area; LA $area_{min}$, minimum left atrial area. RA $area_{max}$, maximum right atrial area; RA $area_{min}$, minimum right atrial area. Data are means ± SEM; Data analyzed by one-way ANOVA with Holm-Sidak post hoc test.

Supplemental Table 2: ECG analysis in male and female db/db mice treated with GLP-1 for 4 weeks.

	wild type	**db/db$_{saline}$**	**db/db$_{GLP-1}$**	***P*** **value db/db$_{saline}$ vs wild type**	***P*** **value db/db$_{GLP-1}$ vs db/db$_{saline}$**	***P*** **value db/db$_{GLP-1}$ vs wild type**
n	25	26	28			
HR (beats/min)	551 ± 8	508 ± 12	536 ± 9	0.007	0.071	0.26
RR interval (ms)	109.4 ± 1.60	120.0 ± 3.1	112.7 ± 1.9	0.006	0.0511	0.32
P wave (ms)	22.7 ± 0.6	30.2 ± 0.9	25.7 ± 0.7	<0.001	<0.001	0.008
PR interval (ms)	36.8 ± 0.5	41.9 ± 1.1	40.3 ± 0.8	<0.001	0.16	0.001
QRS (ms)	10.1 ± 0.4	10.9 ± 0.3	10.4 ± 0.2	0.30	0.63	0.63
QT interval (ms)	54.3 ± 2.2	57.1 ± 2.1	51.4 ± 2.5	0.61	0.22	0.61
cSNRT (ms)	27.4 ± 1.8	40.1 ± 3.5	35.0 ± 1.7	0.001	0.14	0.041
AERP (ms)	29.3 ± 0.8	35.0 ± 0.8	29.5 ± 0.9	<0.001	<0.001	0.89
AVERP (ms)	45.4 ± 1.2	47.6 ± 1.3	44.7 ± 1.6	0.48	0.36	0.70

n, sample size; HR, heart rate; cSNRT, corrected sinoatrial node recovery time; AERP, atrial effective refractory period; AVERP, AV node effective refractory period. Data analyzed by one-way ANOVA with Holm-Sidak post hoc test.

Supplemental Table 3: ECG analysis in female db/db mice treated with GLP-1 for 4 weeks.

	wild type	**db/db$_{saline}$**	**db/db$_{GLP-1}$**	***P*** **value db/db$_{saline}$ vs wild type**	***P*** **value db/db$_{GLP-1}$ vs db/db$_{saline}$**	***P*** **value db/db$_{GLP-1}$ vs wild type**
n	20	17	17			
HR (beats/min)	548 ± 9	497 ± 15	529 ± 12	0.009	0.13	0.25
RR interval (ms)	110.0 ± 1.8	122.7 ± 4.1	114.3 ± 2.6	0.009	0.10	0.30
P wave (ms)	22.5 ± 0.7	29.5 ± 1.1	25.5 ± 1.0	<0.001	0.009	0.023
PR interval (ms)	37.1 ± 0.6	40.5 ± 1.2	40.1 ± .1.2	0.065	0.79	0.065
QRS (ms)	10.0 ± 0.4	10.4 ± 0.4	10.3 ± 0.4	0.88	0.88	0.88
QT interval (ms)	55.7 ± 2.6	59.3 ± 2.7	54.0 ± 3.8	0.64	0.56	0.69
cSNRT (ms)	32.6 ± 3.6	47.0 ± 4.1	43.8 ± 4.4	0.045	0.59	0.10
AERP (ms)	29.7 ± 0.9	35.1 ± 1.2	29.1 ± 1.4	0.004	0.004	0.70
AVERP (ms)	45.5 ± 1.4	47.4 ± 1.8	46.0 ± 2.4	0.83	0.84	0.84

n, sample size; HR, heart rate; cSNRT, corrected sinoatrial node recovery time; AERP, atrial effective refractory period; AVERP, AV node effective refractory period. Data analyzed by one-way ANOVA with Holm-Sidak post hoc test.

Supplemental Table 4: ECG analysis in male db/db mice treated with GLP-1 for 4 weeks.

	wild type	**db/db$_{saline}$**	**db/db$_{GLP-1}$**	***P*** **value db/db$_{saline}$ vs wild type**	***P*** **value db/db$_{GLP-1}$ vs db/db$_{saline}$**	***P*** **value db/db$_{GLP-1}$ vs wild type**
n	5	9	11			
HR (beats/min)	563 ± 18	528 ± 19	548 ± 13	0.50	0.60	0.60
RR interval (ms)	107.0 ± 3.3	114.9 ± 4.3	110.1 ± 2.7	0.46	0.54	0.58
P wave (ms)	23.6 ± 0.9	31.4 ± 2.0	26.0 ± 0.9	0.009	0.019	0.28
PR interval (ms)	35.7 ± 0.8	43.8 ± 1.8	41.2 ± 1.1	0.015	0.191	0.078
QRS (ms)	10.2 ± 1.2	11.6 ± 0.6	10.6 ± 0.3	0.36	0.36	0.64
QT interval (ms)	48.8 ± 1.9	53.1 ± 3.2	47.4 ± 2.3	0.58	0.34	0.74
cSNRT (ms)	25.9 ± 5.9	55.4 ± 8.8	42.4 ± 5.4	0.056	0.29	0.29
AERP (ms)	27.5 ± 1.4	34.9 ± 0.5	30.2 ± 1.1	0.001	0.003	0.13
AVERP (ms)	45.3 ± 2.7	48.0 ± 2.0	42.8 ± 1.8	0.6914	0.20	0.69

n, sample size; HR, heart rate; cSNRT, corrected sinoatrial node recovery time; AERP, atrial effective refractory period; AVERP, AV node effective refractory period. Data analyzed by one-way ANOVA with Holm-Sidak post hoc test.

Supplemental Table 5: ECG analysis in db/db mice treated with liraglutide for 4 weeks.

	wild type	**db/db$_{veh}$**	**db/db$_{lira}$**	***P*** **value db/db$_{veh}$ vs wild type**	***P*** **value db/db$_{lira}$ vs db/db$_{veh}$**	***P*** **value db/db$_{lira}$ vs wild type**
n	13	16	11			
HR (beats/min)	539 ± 9	497 ± 14	523 ± 7	0.033	0.22	0.36
RR interval (ms)	111.8 ± 1.9	122.2 ± 3.7	115.0 ± 1.4	0.039	0.16	0.16
P wave (ms)	22.8 ± 1.1	29.7 ± 0.7	23.7 ± 1.2	<0.001	<0.001	0.56
PR interval (ms)	38.5 ± 0.7	46.0 ± 1.2	43.8 ± 1.1	<0.001	0.16	0.003
QRS (ms)	9.9 ± 0.5	10.7 ± 0.4	9.6 ± 0.4	0.33	0.20	0.60
QT interval (ms)	53.4 ± 2.2	56.9 ± 2.9	57.5 ± 2.0	0.88	0.88	0.88
cSNRT (ms)	25.8 ± 1.8	44.5 ± 3.3	39.5 ± 3.6	<0.001	0.25	0.009
AERP (ms)	29.6 ± 1.0	46.9 ± 3.8	39.2 ± 2.0	<0.001	0.067	0.063
AVERP (ms)	46.6 ± 1.5	53.5 ± 1.9	47.1 ± 1.4	0.015	0.025	0.83

n, sample size; HR, heart rate; cSNRT, corrected sinoatrial node recovery time; AERP, atrial effective refractory period; AVERP, AV node effective refractory period. Data analyzed by one-way ANOVA with Holm-Sidak post hoc test.

Supplemental Table 6: I_{Na} steady-state activation and inactivation parameters in db/db mcie treated with GLP-1 for 4 weeks.

	wild type	**db/db$_{saline}$**	**db/db$_{GLP-1}$**	***P*** **value db/db$_{saline}$ vs wild type**	***P*** **value db/db$_{GLP-1}$ vs db/db$_{saline}$**	***P*** **value db/db$_{GLP-1}$ vs wild type**
n (N)	10 (3)	11 (4)	11 (3)			
G_{max} (pS/pF)	1382.3 ± 106.4	1385.0 ± 106.8	1332.7 ± 112.8	0.99	0.98	0.98
$V_{1/2(act)}$ (mV)	−53.2 ± 1.6	−52.1 ± 1.4	−51.8 ± 1.5	0.89	0.91	0.89
$k_{(act)}$ (mV)	3.4 ± 0.3	4.1 ± 0.4	3.9 ± 0.2	0.38	0.65	0.46
$V_{1/2(inact)}$ (mV)	−82.0 ± 1.3	−75.8 ± 1.3	−81.5 ± 1.0	0.003	0.004	0.78
$k_{(inact)}$ (mV)	−6.1 ± 0.6	−6.0 ± 0.4	−6.1 ± 0.4	>0.99	>0.99	>0.99

n (N), number of cells (number of mice), G_{max}, maximum conductance; $V_{1/2(act)}$, voltage at which 50% of channels are activated; $k_{(act)}$, activation curve slope factor; $V_{1/2(inact)}$, voltage at which 50% of channels are inactivated; $k_{(inact)}$, inactivation curve slope factor. Data analyzed by one-way ANOVA with Holm-Sidak post hoc test, n = 10 cells from 3 mice for wild type, 11 cells from 4 mice for db/db$_{saline}$, and 11 cells from 3 mice for db/db$_{GLP-1}$.

Supplemental Table 7: PCR primers

Gene	**Gene product**	**Primer Sequence (5'→ 3')**	**Amplicon length (bp)**
Kcnd2	K_V4.2	Forward: GCAAGCGGAATGGGCTAC Reverse: TGGTTTTCTCCAGGCAGTG	126
Kcnd3	K_V4.3	Forward: CCTAGCTCCAGCGGACAAGA Reverse: CCACTTACGTTGAGGACGATCA	60
Kcnip 2	KChIP2	Forward: AACTATCCACGGTGTGCCAC Reverse: GGACATTCGTTCTTGAAGCCT	112
Kcna5	K_V1.5	Forward: TTATTCTTATGGCTGACGAGTGC Reverse: AAGGCACCAATAGTACATCCCAG	204
Col1a	Collagen type I	Forward: GCGGACTCTGTTGCTGCTTGC Reverse: GACCTGCGGGACCCCTTTGT	125
Col3a	Collagen type III	Forward: AGATCCGGGTCCTCCTGGCATTC Reverse: CTGGTCCCGGATAGCCACCCAT	194
Hprt1	Hypoxanthine phosphoribosyltransferase 1	Forward: GCAGGTCAGCAAAGAACTTATAGCC Reverse: CTCATGGACTGATTATGGACAGGAC	123